Editors' Suggestion

Spin texture of α-GeTe in the ultrathin regime

Calvin Tagne-Kaegom,[1] Alexandre Llopez,[2] Boris Croes,[2,*] Geoffroy Kremer,[1] Bertrand Kierren,[1] Daniel Malterre,[1] Luc Moreau,[1] Jaurès Fotié Ngoufo,[2] Stefano Curiotto,[2] Pierre Müller,[2] Patrick Le Fèvre,[3,‡] Julien Rault,[3] François Bertran,[3] Andrés Saúl,[2] Frédéric Leroy,[2] Fabien Cheynis,[2,†] and Yannick Fagot-Revurat[1]

[1]*Université de Lorraine, CNRS, Institut Jean Lamour, 54000 Nancy, France*

[2]*Aix Marseille Univ., CNRS, CINAM, AMUtech, Marseille, France*

[3]*Synchrotron SOLEIL, L'Orme des Merisiers, Départementale 128, F-91190 Saint-Aubin, France*

(Received 21 September 2025; accepted 3 February 2026; published 9 March 2026)

Using spin- and angle-resolved photoemission spectroscopy combined with density functional theory calculations, we investigate the electronic structure of α-GeTe grown on a Si(111)-Sb substrate in the ultrathin limit. The full band structure, including the Fermi surface, and spin texture characterizations are presented, with a focus on a film thickness of 5 nm. Well-defined spin-polarized quantum well bulk states are evidenced. This confirms the high quality of elaborated ultrathin films and allows precise determination of the thickness. The Rashba splitting and the in-plane spin texture of GeTe bulk bands are shown to be fully preserved on the Si(111)-Sb substrate. This suggests the persistence of inversion symmetry breaking and ferroelectric properties in the ultrathin limit of GeTe films. Our results demonstrate that device downscaling can be pursued in the context of all-electrically controlled spin-orbitronics applications.

DOI: 10.1103/yst7-ktp9

I. INTRODUCTION

The Rashba effect originates from a combination of spin-orbit coupling and broken symmetry [1,2] at a crystal surface (e.g., metallic surfaces such as Au(111) [3] and surface alloys such as Bi/Ag(111) and Pb/Ag(111) [4,5]), at an interface (e.g., GaAs/AlGaAs(110) quantum well [6], InAs/GaAs semiconducting [7], and Au/W(110) metallic [8] interfaces), or in bulk materials such as BiTeI [9,10]. A dynamic field called spin-orbitronics, aiming at spin-dependent and controllable transport properties for next-generation low-consumption electronics [11–13], has recently emerged. In particular, the spin-to-charge conversion (SCC) phenomenon [14] opens a new route for spintronics applications based on the utilization of the Rashba effect [15,16].

α-GeTe was recently pointed out as a ferroelectric Rashba semiconductor (FERSC), defining a new exciting family of multifunctional materials. Indeed, below its bulk Curie temperature ($T_C = 720$ K), it shows a ferroelectric ordering characterized by a displacement of Te atoms with respect to the central position of the rhombohedral unit cells along the [111] direction. This results in an inversion symmetry breaking in the bulk material and a Rashba-like spin splitting of the electronic band structure related to the ferroelectric configuration [17]. The possible control of this giant Rashba effect was predicted [18] and experimentally evidenced [19,20] along with an effective spin-to-charge conversion at room temperature [13,21]. α-GeTe(111) films have been epitaxially grown on various substrates, such as BaF_2 [22–25], Si(111) [19,26,27], and InP(111) [28]. Bulk α-GeTe single crystals have been also studied [29]. The α-GeTe band structure has been investigated mainly using spin- and angle-resolved photoemission spectroscopy (SR-ARPES) and density functional theory (DFT) calculations, revealing a superposition of spin-polarized bulk and surface bands along with resonant surface states [22]. Moreover, bulk states have been shown to be spin polarized [23,30], and surface states have been fully resolved by doping GeTe films with alkali atoms [29,30] and were recently confirmed by time-resolved ARPES measurements [24,31]. In addition, nontrivial topologies have revealed the occurrence of type-II Weyl and triple-point fermions, which have been pointed out as potential platforms for realizing topological quantum computing [32]. Doping by ferromagnetic Mn impurities allows us to extend the FERSC concept to multiferroic Rashba semiconductors [20,30,33]. Finally, more recent time-resolved ARPES measurements demonstrated the ultrafast light-induced modulation of ferroelectricity [25]. These works open a route to nonvolatile control of spin currents in GeTe-based heterostructures. Nevertheless, the integration of such FERSC materials into nonvolatile memory devices requires one to maintain these functionalities down to the nanometer scale. This raises the question of the persistence of ferroelectrically controllable Rashba coupling for low material thicknesses [34,35].

Until recently, a single work had investigated the thickness dependence of the electronic structure of α-GeTe films. Yang *et al.* [26] showed that for depositions on Si(111), 5 nm GeTe films exhibit a Rashba constant reduced by a factor of 2 with respect to the bulk value. They also pointed out a critical thickness of 2.1 ± 0.5 nm, below which the Rashba spin splitting of the band structure vanishes. This has been interpreted as being a consequence of the restoration of an inversion center

*Present address: Université de Strasbourg, CNRS, IPCMS, UMR 7504, F-67000 Strasbourg, France.

†Contact author: fabien.cheynis@univ-amu.fr

‡Present address: Université Rennes, IPR, UMR 6251, CNRS, F-35000 Rennes, France.

in the atomic structure (i.e., $R3m$ to $R3\bar{m}$ symmetry transition), implying the disappearance of the ferroelectric properties and the Rashba effect in the ultrathin limit. In previous studies, we investigated the early-stage growth regime [27] and the ferroelectric domain structure [36–39] of α-GeTe(111) films deposited by molecular beam epitaxy on Si(111) using a Sb seed layer as initially proposed by Wang *et al.* [40]. Recently, we demonstrated that a giant Rashba effect can be maintained in α-GeTe(111) ultrathin films deposited on Si(111)-Sb down to 1 nm. The crucial role of interfacial Sb atoms in the persistence of spin splitting of the band structure in this thickness regime is discussed in detail in Ref. [41]. However, the spin polarization and spin texture of GeTe films have not been experimentally evidenced in the ultrathin regime. In the present work, we fully characterize the spin-resolved electronic band structure of 5 nm GeTe(111) films deposited on Si(111)-Sb [denoted GeTe(111)-Sb in the following] by combining ARPES and SR-ARPES and *ab initio* calculations. Using well-defined quantized bulk states as a probe of the precise film thickness, we confirm the persistence of spin polarization and spin texture in 5 nm thick GeTe(111)-Sb at the Fermi level, which appears to be ideally suited for spin-orbitronics applications.

II. METHODS

Ultrathin α-GeTe(111) layers have been elaborated on a Si(111)-$\sqrt{3}\times\sqrt{3}$-Sb reconstructed surface following the method described in Ref. [27] (see Sec. 1 of the Supplemental Material for details on the sample preparation [42]). Indeed, the interfacial Sb monolayer has been shown to act as a surfactant during growth up to 5 nm, which promotes high crystallinity and preserves the giant Rashba effect [41]. ARPES and SR-ARPES measurements have been performed at the CASSIOPEE beamline (SOLEIL synchrotron radiation facility, France) on ultrathin GeTe(111)-Sb films capped by a Te layer a few tens of nanometers thick to protect the surface from oxidation during the transfer from the growth chamber to the photoemission chamber (see Sec. 2 in the Supplemental Material [42]). The procedure for the removal of the Te layer to recover a clean α-GeTe(111) surface is described in Sec. 1 of the Supplemental Material. ARPES and SR-ARPES characterizations were also performed on samples transported in a UHV suitcase, leading to the same high-quality experimental results. *Ab initio* calculations were carried out within the DFT framework using the quantum espresso package based on the plane wave basis [43,44]. The generalized gradient approximation with the Perdew-Burke-Ernzerhof exchange-correlation functional [45] and fully relativistic ultrasoft pseudopotentials from pslibrary [46] were employed. Details of the methodology to determine the isoenergy contours and the spin texture of the electronic band structure of a 5 nm GeTe(111) film are given in Sec. 3 of the Supplemental Material [42].

III. RESULTS

A. Band structure in bulk vs ultrathin α-GeTe(111)

We started our investigations on thick GeTe(111)-Sb samples (i.e., $\geqslant$40 nm) in order to validate the electronic band structure with respect to previous works on bulk GeTe(111) [19,22,23]. As shown in Fig. S1 of the Supplemental Material [42], GeTe bulk bands progressively shift downwards in binding energy as the photon energy is increased. A photon energy of 25 eV was then chosen to ensure a clear separation of bulk and surface states in energy with a strong spectral weight on bulk states close to the $\bar{\Gamma}$ point, where the Rashba coupling is the strongest [22]. From the Supplemental Material of Ref. [47], this photon energy corresponds to a k_z point located between the Z and Γ points in the three-dimensional (3D) Brillouin zone. More specifically, using an inner potential of 15 eV, we derive a k_z component of 3.05 Å^{-1} at normal incidence for electrons with a kinetic energy of 20.5 eV. Considering that $||\Gamma - Z|| = 0.93$ Å^{-1}, k_z probed components are typically located 0.63 Å^{-1} below the high-symmetry point Γ of the third Brillouin zone. ARPES intensity maps along the $\bar{\Gamma}$-$\bar{K}$ high-symmetry direction of the hexagonal surface Brillouin zone are shown in Figs. 1(a) and 1(a'). ARPES intensity measured in the $\bar{\Gamma}$-$\bar{K}$ high-symmetry direction exhibits all the spectroscopic signatures of a clean Te-terminated surface: (1) Bulk bands, labeled B_1 and B_2 (red lines), are identified close to the Fermi level. (2) Surface bands, labeled S_1 and S_2 (yellow lines), are visible below the Fermi level at k values > 0.2 Å^{-1}. More precisely, we determine from Fig. 1(a) that the Fermi wave vectors of the S_1 and S_2 surface states are $k_{S_1} = 0.40$ Å^{-1} and $k_{S_2} = 0.27$ Å^{-1}. This band structure is in good agreement with experiments from the literature and calculations performed on α-GeTe(111) [41] and confirms that 40 nm GeTe(111)-Sb films show bulklike properties. The nature of electronic bands (i.e., bulk or surface) can be determined by their photon-energy dependence: Bulk states disperse as a function of the photon energy [i.e., as a function of $k_z(h\nu)$, where k_z is the wave vector component perpendicular to the sample surface], while surface states do not evolve (see Fig. S1 in the Supplemental Material for details [42]). As previously shown in [23], a highly intense surface resonance state crosses the B_1 and B_2 bulk states close to $E_B = 0.25$ eV [Fig. 1(a')]. From Fig. 1(a), we determine a Rashba energy $E_R = 0.3$ eV and a splitting wave vector $k_0 = 0.14$ Å^{-1} for bulk states, leading to a value of the Rashba constant of $\alpha_R = 2E_R/k_0 = 4.9 \pm 0.5$ eV Å, in very good agreement with previous reports for thicker [22,25,26,47] and thinner [41] films. As expected, this Rashba effect related constant is very high compared to those of other systems, such as Au(111), Bi/Ag(111) alloys, and InAS/GaAs heterostructures [3–5,7,16,48].

Let us now discuss the evolution of the electronic band structure after the film thickness is reduced to 5 nm. Although few-nanometer thicknesses might appear at first to be bulklike samples, 5 nm GeTe/Si(111) films already showed a significant reduction of the Rashba effect by a factor of 2 in Ref. [26]. In Ref. [41], we demonstrated, on the other hand, that the surfactant effect of Sb atoms is already at work in 5 nm GeTe/Si(111)-Sb, resulting in an unchanged Rashba constant. Consequently, 5 nm GeTe films can be considered representative of the ultrathin regime where finite size effects are observable. The corresponding ARPES measurements and DFT calculations are presented in Figs. 1(b), (1b'), and 1(b"). Figure 1(b') shows the second derivative of Fig. 1(b) to facilitate the interpretation of the experimental band structure. Several modifications in the band structure can be noted. First,

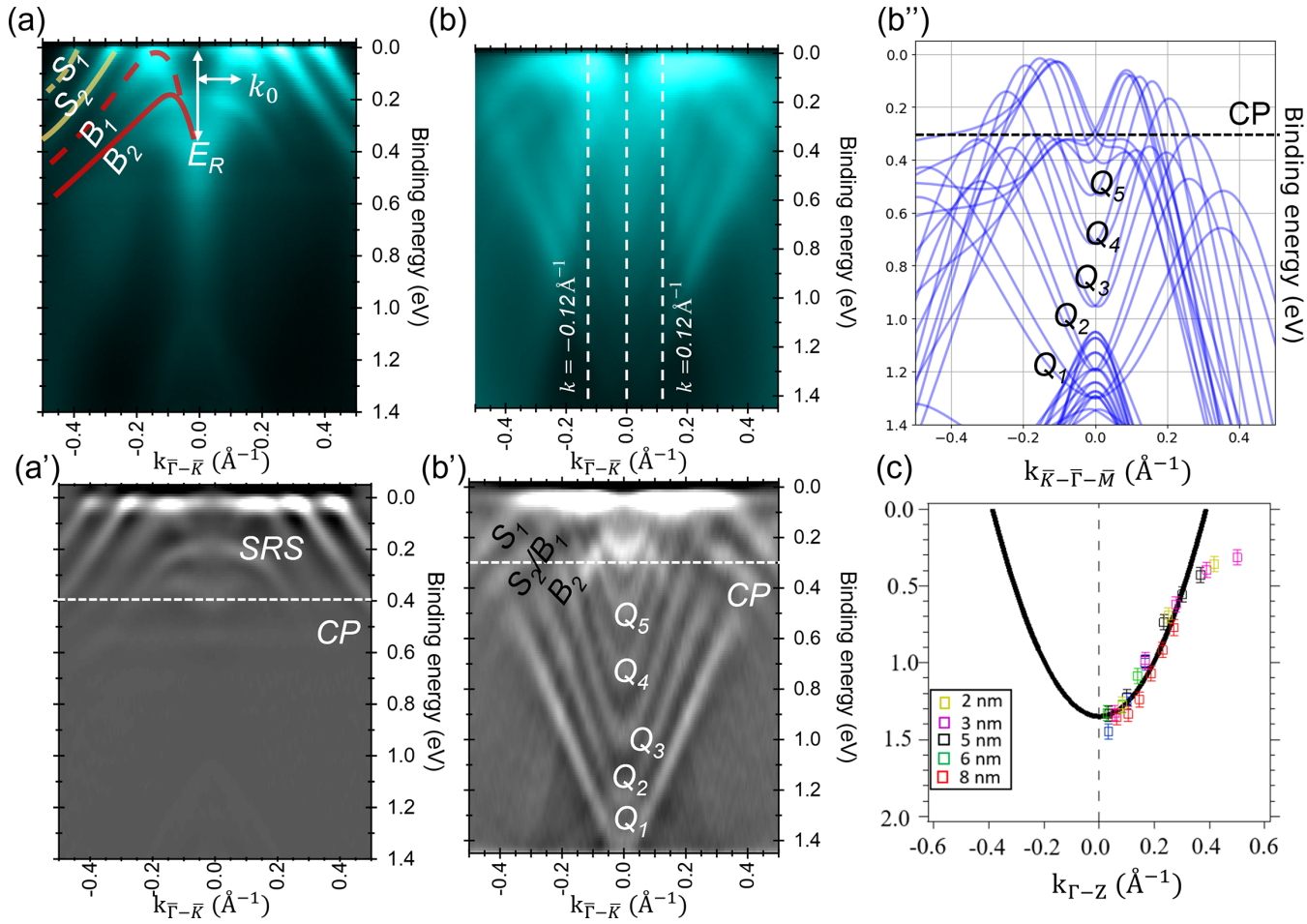

FIG. 1. Comparison of ARPES spectra and DFT calculations. ARPES spectra obtained along the $\bar{\Gamma}$-$\bar{K}$ high-symmetry path of (a) and (a') 40 nm and (b) and (b') 5 nm GeTe(111)-Sb films. White dashed lines in (b) correspond to the energy dispersion curves shown in Fig. 3. (a') and (b') are the second derivatives of the spectra shown in (a) and (b), respectively. Surface (S_1 and S_2) and bulk states (B_1 and B_2) appear in yellow and red, respectively. Q_i labels indicate discrete states originating from the broad continuum in (a) and (a'). (b'') DFT calculation along the K-$\bar{\Gamma}$-$\bar{M}$ high-symmetry path of the electronic band structure of a 5 nm thick GeTe(111) film. (c) Energy dispersion law of the discrete states in the Γ-Z direction (i.e., in the direction of the growth direction). The quadratic numerical fit (solid black line) confirms their quantum well origin.

by comparing Figs. 1(a) and 1(a') with Figs. 1(b) and 1(b'), we can identify only three holelike bands close to the Fermi level in Fig. 1(b'), although four were previously discussed (S_1, S_2, B_1, and B_2). Second, the diffuse bulk continuum below the B_1 and B_2 bulk states has evolved into well-defined quantum well (QW) states, labeled Q_1–Q_5, that are visible in Figs. 1(b') and 1(b'')). This allows for a precise determination of the film thickness (see Fig. S2 in the Supplemental Material for a comparison in which three QW states are visible for a 3 nm GeTe film [42]). DFT calculations also show that these QW states exhibit a Rashba-like degeneracy lift, as evidenced by the two close bands that compose all QWs in Fig. 1(b''). Finally, the surface resonance disappears in the 5 nm thick GeTe film.

To understand the reduction in the number of observed bands between bulklike and 5 nm GeTe(111)-Sb films, we examined the energy position of the crossing point (CP) of the spin-split bulk bands in both samples [see dashed white lines in Figs. 1(a') and 1(b')]. It turns out that, as the film thickness is reduced, the CP is shifted toward lower binding energies by $\simeq$0.1 eV. This value is comparable to the binding energy difference determined for any given k value between S_2 and B_1 states in Figs. 1(a) and 1(a'). As a result, we can assume that bulk states are rigidly shifted toward lower binding energies. The S_2 surface and B_1 bulk states then get closer in the low-thickness regime and form a broad, diffuse band. The origin of this interfacial effect remains to be investigated. From the observed shift of bulk states toward lower binding energies, we expect an increase in the carrier density at the Fermi level for this k_z point. As bulk states in α-GeTe are spin polarized, we anticipate that the controllable spin-charge conversion reported in Ref. [13] could also be modified by adjusting the GeTe film thickness and the density of free carriers available at the Fermi level.

Another noticeable difference between a 5 nm thick GeTe(111)-Sb film and a bulklike sample is the occurrence of discrete states for binding energies higher than 0.3 eV below the Fermi level. QW states and related quantum size effects have been predicted, observed, and analyzed by photoemission since the late 1980s, as reviewed in Ref. [49]. To confirm the physical origin of the discrete states observed for GeTe films thinner than 10 nm (see Fig. S2 in the Sup-

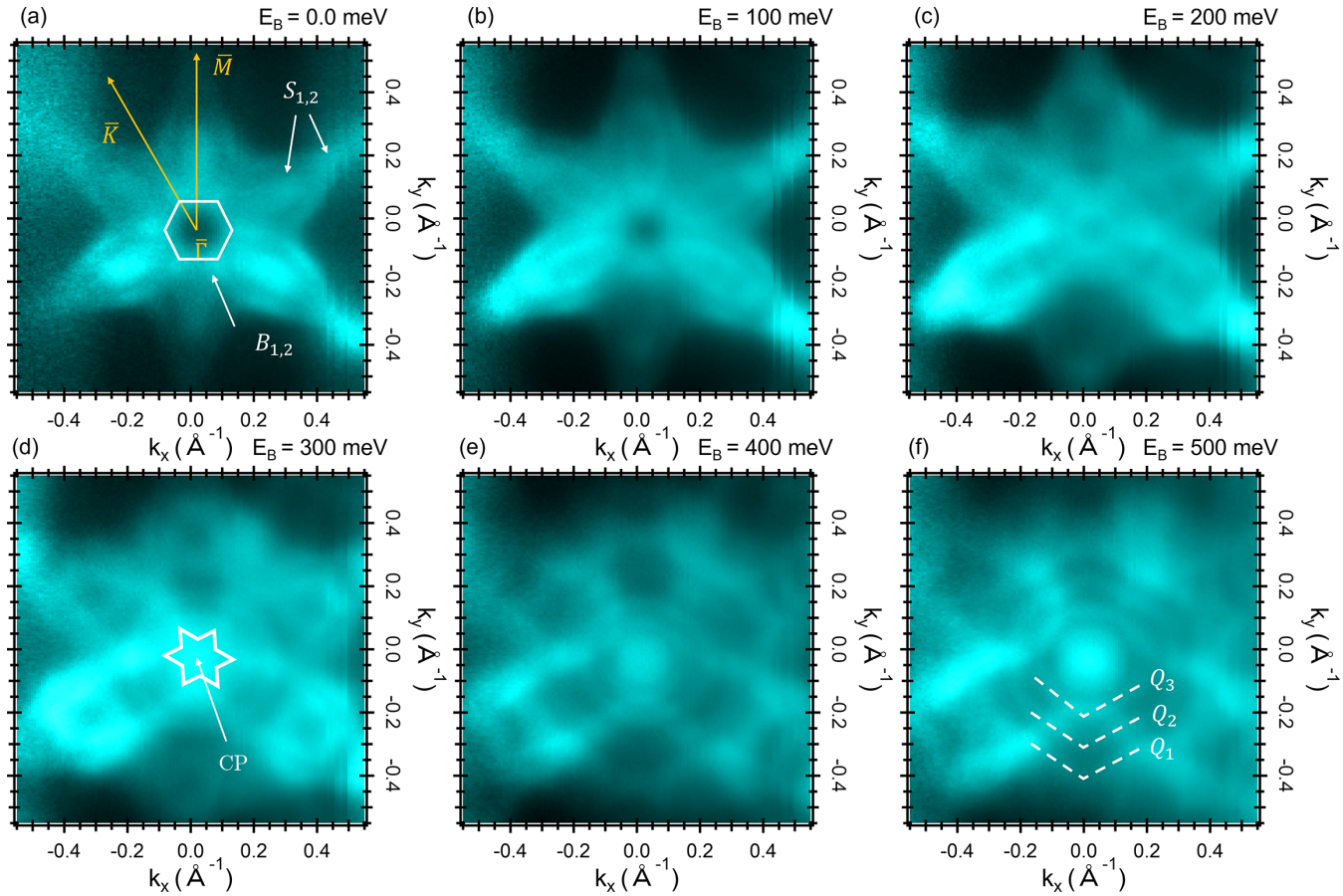

FIG. 2. Isoenergy contours of the electronic band structure of a 5 nm GeTe(111)-Sb thin film for increasing binding energies ($h\nu = 25$ eV). High-symmetry directions are indicated in yellow. White labels indicate surface (S_1 and S_2), bulk (B_1 and B_2), and QW (Q_i) states. See text for details.

plemental Material for a similar characterization of a 3 nm thick GeTe(111)-Sb [42]), we modeled the effect of finite film thicknesses using electronic wave functions confined in the growth direction due to the occurrence of a potential well at the surface or interface. For a free fermion gas confined in the z direction, the energy dispersion law simply reads $E_{n_z} = E_0 + \frac{\hbar^2}{2m^\star}k_{n_z}^2$, where E_0 is an offset energy, $m^\star$ is the electron effective mass, and $k_{n_z} = n_z\pi/L$ is the z component of the electron wave vector defined by its quantum number n_z and the film thickness L. We measured, for different film thicknesses, the energy minimum of the varying number of QW states, from which we can derive the corresponding k_z component of the electronic wavevector in the Γ-Z direction. Figure 1(c) shows the best numerical fit of the experimental data. Below $|k_z| = 0.4\,\text{Å}^{-1}$, the dispersion law is clearly quadratic and confirms that, in the Γ-Z direction, the electrons behave as free carriers confined in a QW. From the curvature of the numerical fit, we derive an effective electron mass of $m^*_{e,\Gamma-Z} = 0.31m_e$.

Recently, the 3D limit of the bulk Rashba effect was studied in GeTe ultrathin films on Si(111) [26] and on Si(111)-Sb [41]. The former work evidenced a reduction of the Rashba effect, with a complete disappearance below a critical thickness close to 2 nm. The authors showed that for a thickness of 5 nm, α_R is reduced with respect to the bulk value of $\alpha_R > 4.5$ eV Å but maintains a value of $\alpha_R = 2.12$ eV Å. In the current work, a Rashba coupling of $\alpha_R = 4.3 \pm 0.5$ eV Å ($\alpha_R = 4.5 \pm 0.3$ eV Å) is determined from ARPES measurements (DFT calculations). These values are slightly lower than the Rashba coefficient of 4.9 ± 0.5 eV Å measured for thick films (>40 nm) and ultrathin GeTe(111)-Sb films [41] but almost 2 times higher than the value reported by Yang *et al.* [26].

To further characterize the band structure of a GeTe(111)-Sb film of reduced thickness, we measured a series of isoenergy contours, as shown in Fig. 2. The Fermi surface of the band structure exhibits a starlike shape, with branches along the $\bar{\Gamma}$-$\bar{M}$ directions and a hexagonal contour in the vicinity of $\bar{\Gamma}$. By comparing this Fermi surface with the ARPES spectrum presented in Figs. 1(b) and 1(b'), we can deduce that the states at the edge of the hexagon ($k \leqslant 0.2\,\text{Å}^{-1}$) mostly correspond to bulk states. The edges of the sixfold star in Fig. 2(a) correspond to the S_1 surface state, and the spectral weight inside this star results from the S_2 and B_1 states. The Fermi surface measured on thick samples (see Fig. S3 in the Supplemental Material for a comparison [42]) or reported in the literature [19,23,28,29] does not show any spectral weight inside the star branches along the $\bar{\Gamma}$-$\bar{M}$ directions. This is in clear disagreement with Fig. 2(a), which exhibits additional occupied states that probably result from the superposition of the contributions from the surface S_2 and bulk B_1 states evidenced earlier. As the binding energy increases, the diameter of the central hexagon diminishes until it vanishes in the vicinity of

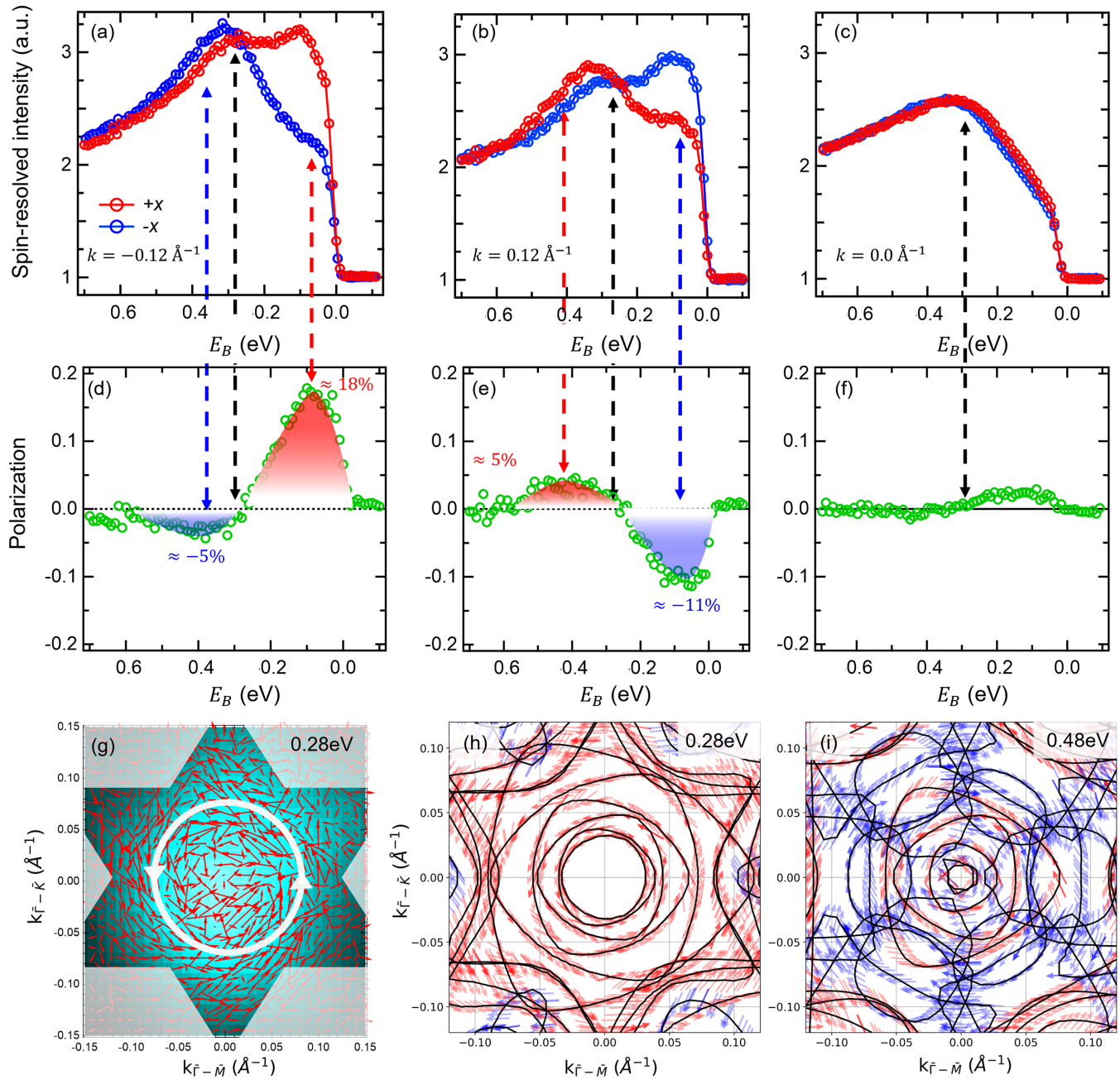

FIG. 3. Spin texture of a 5 nm GeTe/Si(111)-Sb film. Spin-polarized EDCs along the x direction performed at fixed wave vectors (a) $k_{\bar{\Gamma}-\bar{K}} = -0.12$ Å^{-1}, (b) $k_{\bar{\Gamma}-\bar{K}} = 0.12$ Å^{-1}, and (c) $k_{\bar{\Gamma}-\bar{K}} = 0.0$ Å^{-1}. Blue and red dashed lines indicate the energy positions of the spin polarization maxima. Black dashed lines show crossing points. (d)–(f) Spin polarization along x corresponding to EDCs in (a)–(c). (g) In-plane spin texture map of a 5 nm GeTe/Si(111)-Sb determined by SR-ARPES at a constant energy of $E_B = 0.28$ eV, with red arrows representing the measured spin polarization direction and amplitude. The circular white arrows are a guide to the eye for the overall counterclockwise spin rotation. The color map is a zoom of the isoenergy contour delimited by the white star in Fig. 2(d). Spin texture of the isoenergy contours calculated by DFT at (h) $E_B = 0.28$ eV and (i)$E_B = 0.48$ eV. The spin rotation is reversed when the energy is changed from $E_B = 0.28$ eV to $E_B = 0.48$ eV.

$E_B = 300$ meV [Fig. 2(d)]. This energy corresponds to the CP associated with the intersection of the B_1 and B_2 states at the $\bar{\Gamma}$ point. At higher binding energies, QW states become visible in the shape of concentric hexagons [Figs. 2(e) and 2(f)].

B. Spin texture in ultrathin α-GeTe(111)

The spin polarization and spin texture of GeTe films have been shown to play a crucial role in spintronics application such as SCC [13,21]. To date, only GeTe crystals and bulklike films have been studied [19,20,22,23,32,47,50,51]. The question of the persistence of the spin texture in the ultrathin-film regime is of topical importance for applications and device downscaling. To answer this question, we performed spin-polarized ARPES measurements on 5 nm thick GeTe(111)-Sb films. In particular, we determined energy dispersion curves (EDCs) at three fixed k-component values (Figs. 1 and 3) using ultrasensitive very low energy electron

diffraction (VLEED) spin detection (see details in Sec. 2 of the Supplemental Material [42]): at the $\bar{\Gamma}$ point ($k_{\bar{\Gamma}-\bar{K}} = 0.0$ Å^{-1}) and at $k_{\bar{\Gamma}-\bar{K}} = \pm 0.12$ Å^{-1}. The spin-resolved EDCs along the in-plane x direction ($\bar{\Gamma}$-$\bar{M}$ path) are shown by red and blue curves in Figs. 3(a)–3(c). The corresponding experimental spin polarization S_x, deduced from the asymmetry between the $+x$-spin and $-x$-spin contributions using an effective Sherman function of 0.2, is represented using open green circles in Figs. 3(d)–3(f) that correspond, respectively, to $k = \pm 0.12$ Å^{-1} and 0.0 Å^{-1}. At $k = 0.0$ Å^{-1}, we observe that the $+x$-spin and $-x$-spin EDCs overlap each with other almost perfectly, leading to a total spin polarization close to zero [see Figs. 3(c) and 3(f)]. The residual polarization is likely due to a slight sample misalignment. In addition, the spin-polarized spectra display a unique peak with a maximum located 300 meV below the Fermi level. This can be ascribed to the intersection of electronic bands (the CP mentioned before) and confirms the Rashba energy of $E_R = 300$ meV determined by ARPES measurements. Let us now analyze the spin-polarized EDCs performed at opposite k points ($k_{\bar{\Gamma}-\bar{K}} = \pm 0.12$ Å^{-1}, i.e., close to k-space positions where only bulk bands $B_{1,2}$ are expected to contribute to the photoemission signal). EDCs performed at these k values indeed closely intersect the maxima of the B_1 and B_2 bands, as illustrated by white dashed lines in Fig. 1(b). In Fig. 3(a), the $+x$-spin and $-x$-spin EDCs display two maxima at binding energies of 380 and 80 meV (dashed red arrows), arising from the spin-split B_1 and B_2 bands. More specifically, from 600 to 300 meV, the $-x$-spin EDC intensity (in blue) is slightly higher than the $+x$-spin contribution (in red), leading to a net S_x polarization of -5%, as shown in Fig. 3(d). In other words, the B_2 band is spin polarized along the $-x$ direction for $k_{\bar{\Gamma}-\bar{K}} < 0$ values. From 300 meV to the Fermi level, the $+x$-spin EDC intensity is larger than the $-x$-spin component, leading to a maximum S_x polarization of $+18\,\%$. The S_x polarization of B_1 is thus positive for $k_{\bar{\Gamma}-\bar{K}} < 0$ values. If we compare Figs. 3(a) and 3(c) with Figs. 3(b) and 3(e), a reversal of the spin polarization is clearly observed when moving from $k = -0.12$ Å^{-1} to $k = 0.12$ Å^{-1}, with the net S_x polarization reaching -11%. The observed reversal of the spin polarization when the momentum is inverted with respect to the Brillouin zone center, reported in bulk α-GeTe, strongly suggests that the inversion symmetry breaking in ultrathin 5 nm GeTe films still occurs, as expected from the persistence of the Rashba effect [41].

To confirm this result, we determined the full in-plane spin texture of the Rashba bulk bands at a constant binding energy slightly above the CP (i.e., photoemission intensity vs S_x, S_y, k_x, and k_y at a binding energy of 280 meV), as displayed in Fig. 3(g). The spin components along the x and y directions for each (k_x, k_y) value are displayed as red arrows and superimposed on the Fermi surface zoom of Fig. 2(d). The direction and the length of each arrow represent, respectively, the in-plane components and the magnitude of spin polarization at each k value. We observe a global counterclockwise rotation of the in-plane spin polarization, which is a clear signature of a reminiscent spin texture of the band structure in the ultrathin regime of GeTe/Si(111)-Sb films. The ARPES intensity map determined at the same binding energy appears as a diffuse sixfold star resulting from the superposition of several concentric contours evolving from a ring to stars as the relative size increases in reciprocal space. The spin orientation of the band structure of a 5 nm thick GeTe(111)-Sb film was also determined by DFT calculations [Fig. 3(h)]. The spin texture in the represented reciprocal space region (± 0.12 Å^{-1} around $\bar{\Gamma}$) is almost exclusively counterclockwise, in agreement with SR-ARPES measurements. Both experiments and *ab initio* calculations thus demonstrate the persistence of a spin-textured band structure for 5 nm thick GeTe(111)-Sb films. From the spin-resolved EDCs shown in Figs. 3(a) and 3(b), we also expect a change in the chirality of the band structure spin texture at higher binding energies. We display in Fig. 3(i) the calculated spin texture of the main bulk bands determined for $E_B = 480$ meV (i.e., below the band CP), where the spin polarization indeed rotates mainly clockwise and confirms again the occurrence of a spin texture in the electronic bulk band structure in ultrathin GeTe(111)-Sb films.

IV. CONCLUSION

To summarize, we reported an investigation of the electronic band structure of α-GeTe in its ultrathin limit using SR-ARPES and *ab initio* calculations. We demonstrated an energy shift of the spin-split bulk bands when reducing the thickness down to 5 nm. We showed that the Rashba split bulk states are shifted toward lower binding energies and thus partially merge with the surface states, resulting in a slightly doped film at this thickness. Using SR-ARPES we extracted 18% of the spin polarization, which comes mainly from the bulk states crossing the Fermi level. This makes the conductivity in GeTe at this thickness mainly due to bulk states that happen to be strongly spin polarized, in agreement with the persistence of the giant Rashba splitting. Our results also suggest the persistence of an out-of-plane ferroelectricity in GeTe/Si(111)-Sb down to 5 nm because both the Rashba effect and ferroelectric properties rely on inversion symmetry breaking of the atomic structure. Our study confirms potential routes for technological applications in spintronics, especially in the context of the miniaturization of devices at the nanometer scale.

ACKNOWLEDGMENTS

F.C. is grateful to D. García Ovalle for insightful discussions. The project leading to this publication received funding from the Excellence Initiative of Aix-Marseille University A*MIDEX, a French Investissements d'Avenir program (AMX-22-RE-AB-043) and through the AMUtech Institute. This work was also supported by the ANR grant FETh (Grant No. ANR-22-CE08-0023).

DATA AVAILABILITY

The data that support the findings of this article are not publicly available. The data are available from the authors upon reasonable request.

[1] E. I. Rashba and V. I. Sheka, Symmetry of energy bands in crystals of wurtzite type II. Symmetry of bands with spin-orbit interaction included, New. J. Phys. **17**, 050202 (2015). Originally published in Fiz. Tverd. Tela: Collected Papers **2**, 62 (1959).

[2] Y. A. Bychkov and E. I. Rashba, Properties of a 2D electron-gas with lifted spectral degeneracy, JETP Lett. **39**, 78 (1984).

[3] S. LaShell, B. A. McDougall, and E. Jensen, Spin splitting of an Au (111) surface state band observed with angle resolved photoelectron spectroscopy, Phys. Rev. Lett. **77**, 3419 (1996).

[4] C. R. Ast, J. Henk, A. Ernst, L. Moreschini, M. C. Falub, D. Pacilé, P. Bruno, K. Kern, and M. Grioni, Giant spin splitting through surface alloying, Phys. Rev. Lett. **98**, 186807 (2007).

[5] G. Bihlmayer, S. Blügel, and E. V. Chulkov, Enhanced Rashba spin-orbit splitting in Bi/Ag(111) and Pb/Ag(111) surface alloys from first principles, Phys. Rev. B **75**, 195414 (2007).

[6] G. Wang, A. Balocchi, A. Poshakinskiy, C. Zhu, S. Tarasenko, T. Amand, B. Liu, and X. Marie, Magnetic field effect on electron spin dynamics in (110) GaAs quantum wells, New J. Phys. **16**, 045008 (2014).

[7] J. Nitta, T. Akazaki, H. Takayanagi, and T. Enoki, Gate control of spin-orbit interaction in an inverted $In_{0.53}Ga_{0.47}As/In_{0.52}Al_{0.48}As$ heterostructure, Phys. Rev. Lett. **78**, 1335 (1997).

[8] A. Varykhalov, J. Sánchez-Barriga, A. M. Shikin, W. Gudat, W. Eberhardt, and O. Rader, Quantum cavity for spin due to spin-orbit interaction at a metal boundary, Phys. Rev. Lett. **101**, 256601 (2008).

[9] M. Bahramy, B.-J. Yang, R. Arita, and N. Nagaosa, Emergence of non-centrosymmetric topological insulating phase in BiTeI under pressure, Nat. Commun. **3**, 679 (2012).

[10] K. Ishizaka, *et al.*, Giant Rashba-type spin splitting in bulk BiTeI, Nat. Mater. **10**, 521 (2011).

[11] S. Manipatruni, D. E. Nikonov, C.-C. Lin, T. A. Gosavi, H. Liu, B. Prasad, Y.-L. Huang, E. Bonturim, R. Ramesh, and I. A. Young, Scalable energy-efficient magnetoelectric spin–orbit logic, Nature (London) **565**, 35 (2019).

[12] P. Noël, F. Trier, L. M. Vicente Arche, J. Bréhin, D. C. Vaz, V. Garcia, S. Fusil, A. Barthélémy, L. Vila, M. Bibes, and J.-P. Attané, Non-volatile electric control of spin–charge conversion in a $SrTiO_3$ Rashba system, Nature (London) **580**, 483 (2020).

[13] S. Varotto, L. Nessi, S. Cecchi, J. Sławińska, P. Noël, S. Petrò, F. Fagiani, A. Novati, M. Cantoni, D. Petti, E. Albisetti, M. Costa, R. Calarco, M. B. Nardelli, M. Bibes, S. Picozzi, J.-P. Attané, L. Vila, R. Bertacco, and C. Rinaldi, Room-temperature ferroelectric switching of spin-to-charge conversion in germanium telluride, Nat. Electron. **4**, 740 (2021).

[14] J. R. Sánchez, L. Vila, G. Desfonds, S. Gambarelli, J. Attané, J. De Teresa, C. Magén, and A. Fert, Spin-to-charge conversion using Rashba coupling at the interface between non-magnetic materials, Nat. Commun. **4**, 2944 (2013).

[15] H. Kohno, Spintronics with Weyl semimetal, JPSJ News Comments **18**, 13 (2021).

[16] G. Bihlmayer, P. Noël, D. V. Vyalikh, E. V. Chulkov, and A. Manchon, Rashba-like physics in condensed matter, Nat. Rev. Phys. **4**, 642 (2022).

[17] S. Picozzi, Ferroelectric Rashba semiconductors as a novel class of multifunctional materials, Front. Phys. **2**, 1 (2014).

[18] D. Di Sante, P. Barone, R. Bertacco, and S. Picozzi, Electric control of the giant Rashba effect in bulk GeTe, Adv. Mater. **25**, 509 (2013).

[19] C. Rinaldi, S. Varotto, M. Asa, J. Sławińska, J. Fujii, G. Vinai, S. Cecchi, D. Di Sante, R. Calarco, I. Vobornik, G. Panaccione, S. Picozzi, and R. Bertacco, Ferroelectric control of the spin texture in GeTe, Nano Lett. **18**, 2751 (2018).

[20] J. Krempaský, S. Muff, J. Minár, N. Pilet, M. Fanciulli, A. P. Weber, E. B. Guedes, M. Caputo, E. Müller, V. V. Volobuev, M. Gmitra, C. A. F. Vaz, V. Scagnoli, G. Springholz, and J. H. Dil, *Operando* imaging of all-electric spin texture manipulation in ferroelectric and multiferroic Rashba semiconductors, Phys. Rev. X **8**, 021067 (2018).

[21] C. Rinaldi, *et al.*, Evidence for spin to charge conversion in GeTe (111), APL Mater. **4**, 032501 (2016).

[22] J. Krempaský, H. Volfová, S. Muff, N. Pilet, G. Landolt, M. Radović, M. Shi, D. Kriegner, V. Holý, J. Braun, H. Ebert, F. Bisti, V. A. Rogalev, V. N. Strocov, G. Springholz, J. Minár, and J. H. Dil, Disentangling bulk and surface Rashba effects in ferroelectric α-GeTe, Phys. Rev. B **94**, 205111 (2016).

[23] J. Krempaský, M. Fanciulli, L. Nicolaï, J. Minár, H. Volfová, O. Caha, V. V. Volobuev, J. Sánchez-Barriga, M. Gmitra, K. Yaji, K. Kuroda, S. Shin, F. Komori, G. Springholz, and J. H. Dil, Fully spin-polarized bulk states in ferroelectric GeTe, Phys. Rev. Res. **2**, 013107 (2020).

[24] O. J. Clark, I. Wadgaonkar, F. Freyse, G. Springholz, M. Battiato, and J. Sánchez-Barriga, Ultrafast thermalization pathways of excited bulk and surface states in the ferroelectric Rashba semiconductor GeTe, Adv. Mater. **34**, 2200323 (2022).

[25] G. Kremer, J. Maklar, L. Nicolaï, C. W. Nicholson, C. Yue, C. Silva, P. Werner, J. H. Dil, J. Krempaský, G. Springholz, R. Ernstorfer, J. Minár, L. Rettig, and C. Monney, Field-induced ultrafast modulation of Rashba coupling at room temperature in ferroelectric α-GeTe(111), Nat. Commun. **13**, 6396 (2022).

[26] X. Yang, *et al.*, Three-dimensional limit of bulk Rashba effect in ferroelectric semiconductor GeTe, Nano Lett. **21**, 77 (2021).

[27] B. Croes, F. Cheynis, Y. Fagot-Revurat, P. Müller, S. Curiotto, and F. Leroy, Early-stage growth of GeTe on Si(111)-Sb, Phys. Rev. Mater. **7**, 014409 (2023).

[28] G. Kremer, T. Jaouen, B. Salzmann, L. Nicolaï, M. Rumo, C. W. Nicholson, B. Hildebrand, J. H. Dil, J. Minár, G. Springholz, J. Krempaský, and C. Monney, Unveiling the complete dispersion of the giant Rashba split surface states of ferroelectric α-GeTe(111) by alkali doping, Phys. Rev. Res. **2**, 033115 (2020).

[29] H. Ryu, J.-M. Lihm, J. Cha, B. Kim, B. S. Kim, W. Kyung, I. Song, Y. Kim, G. Han, J. Denlinger, I. Chung, C.-H. Park, S. R. Park, and C. Kim, Chemical control of the Rashba spin splitting size of α-GeTe(111) surface states by adjusting the potential at the topmost atomic layer, Phys. Rev. B **103**, 245113 (2021).

[30] J. Krempaský, G. Springholz, J. Minár, and J. H. Dil, α-GeTe and (GeMn)Te semiconductors: A new paradigm for spintronics, AIP Conf. Proc **1996**, 020026 (2018).

[31] G. Kremer, L. Nicolaï, F. Chassot, J. Maklar, C. W. Nicholson, J. H. Dil, J. Krempaský, G. Springholz, R. Ernstorfer, J. Minár, L. Rettig, and C. Monney, Conduction band structure and ultrafast dynamics of ferroelectric α-GeTe(111), Phys. Rev. B **111**, 235109 (2025).

[32] J. Krempaský, L. Nicolaï, M. Gmitra, H. Chen, M. Fanciulli, E. B. Guedes, M. Caputo, M. Radović, V. V. Volobuev, O. Caha, G. Springholz, J. Minár, and J. H. Dil, Triple-point fermions in ferroelectric GeTe, Phys. Rev. Lett. **126**, 206403 (2021).

[33] J. Krempaský, S. Muff, F. Bisti, M. Fanciulli, H. Volfová, A. P. Weber, N. Pilet, P. Warnicke, H. Ebert, J. Braun, F. Bertran, V. V. Volobuev, J. Minár, G. Springholz, J. H. Dil, and V. N. Strocov, Entanglement and manipulation of the magnetic and spin–orbit order in multiferroic Rashba semiconductors, Nat. Commun. **7**, 13071 (2016).

[34] D. D. Awschalom and M. E. Flatté, Challenges for semiconductor spintronics, Nat. Phys. **3**, 153 (2007).

[35] H. C. Koo, S. B. Kim, H. Kim, T.-E. Park, J. W. Choi, K.-W. Kim, G. Go, J. H. Oh, D.-K. Lee, E.-S. Park, I.-S. Hong, and K.-J. Lee, Rashba effect in functional spintronic devices, Adv. Mater. **32**, 2002117 (2020).

[36] B. Croes, F. Cheynis, Y. Zhang, C. Voulot, K. D. Dorkenoo, S. Cherifi-Hertel, C. Mocuta, M. Texier, T. Cornelius, O. Thomas, M.-I. Richard, P. Müller, S. Curiotto, and F. Leroy, Ferroelectric nanodomains in epitaxial GeTe thin films, Phys. Rev. Mater. **5**, 124415 (2021).

[37] B. Croes, F. Cheynis, P. Müller, S. Curiotto, and F. Leroy, Polar surface of ferroelectric nanodomains in GeTe thin films, Phys. Rev. Mater. **6**, 064407 (2022).

[38] B. Croes, I. Gaponenko, C. Voulot, O. Grégut, K. D. Dorkenoo, F. Cheynis, S. Curiotto, P. Müller, F. Leroy, K. Cordero-Edwards, P. Paruch, and S. Cherifi-Hertel, Automatic ferroelectric domain pattern recognition based on the analysis of localized nonlinear optical responses assisted by machine learning, Adv. Phys. Res. **2**, 2200037 (2023).

[39] B. Croes, F. Cheynis, S. Cherifi-Hertel, K. D. Dorkenoo, P. Müller, S. Curiotto, and F. Leroy, Polarization structure of nanostrip domain intersections in GeTe films, Phys. Rev. B **109**, 024103 (2024).

[40] R. Wang, J. E. Boschker, E. Bruyer, D. Di Sante, S. Picozzi, K. Perumal, A. Giussani, H. Riechert, and R. Calarco, Toward truly single crystalline GeTe films: The relevance of the substrate surface, J. Phys. Chem. C **118**, 29724 (2014).

[41] B. Croes, A. Llopez, C. Tagne-Kaegom, B. Tegomo-Chiogo, B. Kierren, S. Curiotto, P. Müller, A. Saùl, Y. Fagot-Revurat, F. Leroy, and F. Cheynis, Pushing the thickness limit of the giant Rashba effect in ferroelectric semiconductor GeTe, Nano Lett. **24**, 13224 (2024).

[42] See Supplemental Material at http://link.aps.org/supplemental/10.1103/yst7-ktp9 for additional information on the ultrathin GeTe film preparation, ARPES and SR-ARPES measurements, and DFT calculations. The photon energy dependence and isoenergy contours of the electronic band structure of a bulklike GeTe(111)-Sb film determined by ARPES are also provided. The electronic band structure of a 3 nm thick GeTe(111)-Sb obtained from ARPES measurements and DFT calculations is accessible.

[43] P. Giannozzi, *et al.*, QUANTUM ESPRESSO: A modular and open-source software project for quantum simulations of materials, J. Phys.: Condens. Matter **21**, 395502 (2009).

[44] P. Giannozzi, *et al.*, Advanced capabilities for materials modeling with Quantum ESPRESSO, J. Phys.: Condens. Matter **29**, 465901 (2017).

[45] J. P. Perdew, K. Burke, and M. Ernzerhof, Generalized gradient approximation made simple, Phys. Rev. Lett. **77**, 3865 (1996).

[46] A. Dal Corso, Pseudopotentials periodic table: From H to Pu, Comput. Mater. Sci. **95**, 337 (2014).

[47] M. Liebmann, *et al.*, Giant Rashba-type spin splitting in ferroelectric GeTe(111), Adv. Mater. **28**, 560 (2016).

[48] G. Bihlmayer, O. Rader, and R. Winkler, Focus on the Rashba effect, New J. Phys. **17**, 050202 (2015).

[49] T.-C. Chiang, Photoemission studies of quantum well states in thin films, Surf. Sci. Rep. **39**, 181 (2000).

[50] H. J. Elmers, *et al.*, Spin mapping of surface and bulk Rashba states in ferroelectric α-GeTe(111) films, Phys. Rev. B **94**, 201403(R) (2016).

[51] A. S. Frolov, J. Sánchez-Barriga, C. Callaert, J. Hadermann, A. V. Fedorov, D. Y. Usachov, A. N. Chaika, B. C. Walls, K. Zhussupbekov, I. V. Shvets, M. Muntwiler, M. Amati, L. Gregoratti, A. Y. Varykhalov, O. Rader, and L. V. Yashina, Atomic and electronic structure of a multidomain GeTe crystal, ACS Nano **14**, 16576 (2020).